RSC Advances

ROYAL SOCIETY OF CHEMISTRY

www.rsc.org/advances

Aryldihydronaphtalene-type lignans from *Bursera fagaroides* var. *fagaroides* and their antimitotic mechanism of action

Mayra Y. Antúnez Mojica[a], Alejandra León[a], Andrés M. Rojas-Sepúlveda[b], Silvia Marquina[a], Mario A. Mendieta-Serrano[c], Enrique Salas-Vidal[c,*], María Luisa Villarreal[d], Laura Alvarez[a,*]

Corresponding authors

Laura Alvarez

Centro de Investigaciones Químicas-IICBA, Universidad Autónoma del Estado de Morelos. Av. Universidad 1001, Col. Chamilpa, Cuernavaca, Morelos 62209, México

lalvarez@uaem.mx

Phone: +52 777 3297997; +52 777 3079200

Enrique Salas Vidal

Departamento de Genética del Desarrollo y Fisiología Molecular, Instituto de Biotecnología, Universidad Nacional Autónoma de México, A.P. 510-3, Cuernavaca, Morelos 62271, México.

esalas@ibt.unam.mx

Phone: +52 7773291663; Fax: +52 777 3172388

Abstract

Three new aryldihydronaphtalene-type lignans: 7',8'-dehydropodophyllotoxin (**1**), 7',8'-dehydro acetylpodophyllotoxin (**2**) and 7',8'-dehydro *trans-p*-cumaroylpodophyllotoxin (**3**), were isolated from the stem bark of *Bursera fagaroides* var. *fagaroides* (Burseraceae), together with six known lignans, podophyllotoxin (**4**), acetylpodophyllotoxin (**5**), 5'-desmethoxy-β-peltatin A methylether (**6**), acetylpicropodophyllotoxin (**7**), burseranin (**8**), hinokinin (**9**). The coumarin scopoletin (**10**) was also isolated from this bark. The chemical structure of all of these compounds was determined by spectroscopic analyses including 2D NMR. We demonstrated that compounds **1-3** show different degrees of cytotoxic activity against human nasopharyngeal (KB), colon (HF-6), breast (MCF-7) and prostate (PC-3) cancer cell lines, with IC_{50} values ranging from 1.49 to 1.0×10^{-5} μM. *In vivo* studies of the effect of these natural lignans on cell cycle, cell migration and microtubule cytoskeleton of developing zebrafish embryos, demonstrated their antimitotic molecular activity by disturbing tubulin. This is the first report on the occurrence of aryldihydronaphthalene lignans in the genus *Bursera* of the Burseraceae, as well as on the determination of their cytotoxic activity and mechanism of action.

Keywords: aryldihydronaphtalene-type lignans; zebrafish; cytotoxic activity, antimitotic, microtubule cytoskeleton, tubulin.

1. Introduction

Bursera fagaroides (Kunth) Engl, is a small tree that belongs to the genus *Bursera* of the Buseraceae family. *B. fagaroides* is distributed from the United States to south México, and is locally known as "aceitillo", "copal" and "sarzafrás".[1] Its stem bark and exudates are both used in folk medicine to treat hits and tumors. Previous studies have demonstrated its effects on mouse and human spermatozoa immobilization,[2] as well as activities as an amoebicide,[3] immunomodulator and antitumoral medication. [4,5] Previous phytochemical studies showed the presence of podophyllotoxin related lignans in the bark[5,6.] Recently, a bioassay-guided phytochemical investigation revealed the presence of seven aryltetralin-type lignans as the cytotoxic components of the hydroalcoholic extract obtained from the stem bark of this plant.[7] In addition, their antimitotic activity by disturbing tubulin was demonstrated by using the zebrafish embryo model.[8]

In view of the biological importance of compounds obtained from *Bursera*, and in continuation of our search for plant cytotoxic natural compounds,[9-11] we undertook detailed investigation of the dichloromethane extract from the stem bark of *B. fagaroides*. Herein we describe the isolation, and structure elucidation of nine podophyllotoxin-type lignans (**1-9**), together with the coumarin scopoletin (**10**). Compounds **1-3** were new natural products with aryldihydronaphthalene skeleton reported for the first time in the genus *Bursera*. The isolated pure compounds (**1-3**) were assayed for their cytotoxic activity and their effect on cell cycle using the *in vivo* model of zebrafish embryos was determined. The obtained results suggest the necessity of further investigations with the compounds, to develop moieties of therapeutic usefulness.

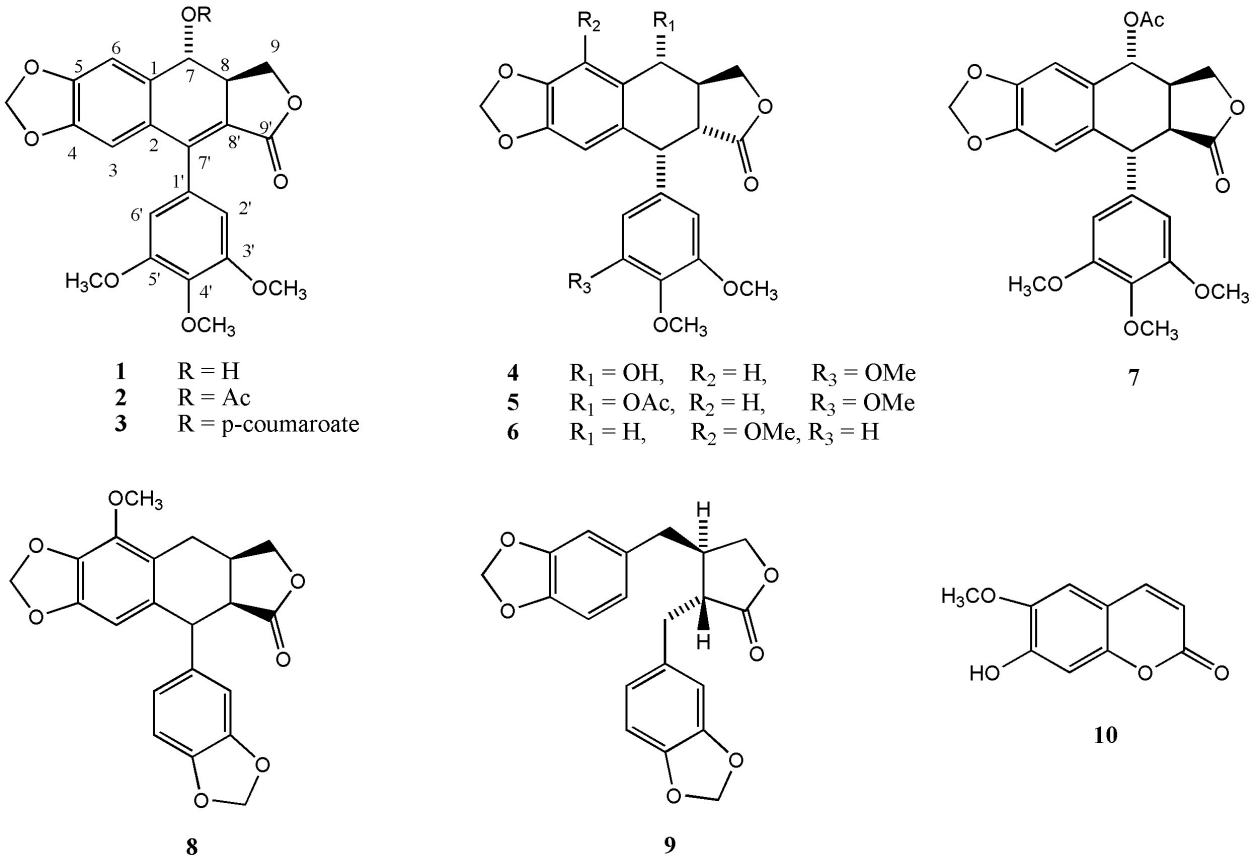

Figure 1. Structures of **1-10** from the stem bark of *B. fagaroides*

2. Results and discussion

In a previous study, the CH_2Cl_2 extract from the stem bark of *Bursera fagaroides* has revealed significant cytotoxic activity against a panel of four cancer cell lines with IC_{50} values ranging from 0.96 to 3.71 μg/mL.[12] Repeated column chromatography resulted in the isolation of three new aryldihydronaphtalene-type lignans named: 7',8'-dehydropodophyllotoxin (**1**), 7',8'-dehydro acetyl podophyllotoxin (**2**), and 7',8'-dehydro-*trans-p*-coumaroyl podophyllotoxin (**3**), together with seven known compounds.

Compound **1** was obtained as an amorphous powder, mp 271-273 °C $[\alpha]^{25}_D$ -95.0 (c 0.090, $CHCl_3$). The HRFABMS of **1** showed the quasimolecular ion peak at *m/z* 413.1301 $[M + H]^+$.

The mass and NMR data (Table 1) provided its molecular formula as $C_{22}H_{21}O_8$ $[M + H]^+$ (calcd for $C_{22}H_{21}O_8$ $[M + H]^+$ 413.1191), indicating 13 degrees of unsaturation. The IR spectrum showed that compound **1** contained absorption bands for hydroxyl (3440.0 cm^{-1}), and ester (1757.5, 1709.3 cm^{-1}) groups, as well as aromatic rings (1633.4, 1608.6, 1588.7 cm^{-1}).

The ^{13}C NMR spectrum (Table 1) displayed the occurrence of 21 carbon resonances ascribable to one carboxyl (δ_C 168.0), one tetrasubstitued double bound (δ_C 147.9, and 118.4), one methylenedioxy group (δ_C 102.0), three methoxyls (δ_C 58.6 (×2), and 61.2), one aliphatic methylene (δ_C 70.1), two aliphatic methines (δ_C 74.2, and 43.9), and 12 aromatic carbons (δ_C 102.0 – 152.4) due to two benzene rings.

The ^1H NMR spectrum (Table 1) showed signals of one unsymmetrical 1,2,4,5-tetrasubstituted [δ_H 7.2, 1H, s, and 6.52, 1H, s], and one symmetrical 1,3,4,5-tetrasubstituted (δ_H 6.52, 2H, s) aromatic rings, one oxygenated methine [δ_H 4.89, 1H, d, J = 14.0 Hz], one oxygenated methylene [δ_H 4.76 (1H, dd, J = 9.2, 9.0 Hz), and 4.26 (1H, dd, J = 9.6, 8.4 Hz)], three methoxyls [δ_H 3.92 (3H, s), and 3.75 (6H, s)], and one methylenedioxy [δ_H 5.991 (1H, d, J = 0.8 Hz), 5.998 (1H, d, J = 0.8 Hz)]. The ^1H-NMR (Table 1) and $^1H/^1H$COSY spectra revealed the presence of a 7',8'-dihydronaphtalene-type lignan skeleton by the four proton spin system [δ_H 4.89 (1H, d, J = 14.0 Hz, H-7), 4.76 (1H, dd, J = 9.2, 9.0 Hz, H-9a), 4.26 (1H, dd, J = 9.6, 8.4 Hz, H-9b), and 3.37 (1H, dt, J = 14.0, 8.4 Hz, H-8)] (Figure 1), which was supported by the three aliphatic resonances in the ^{13}C NMR spectrum [δ_C 74.2 (CH, C-7), 43.9 (CH, C-8), 70.1 (CH_2, C-9)], as well as by the presence of a tetrasubstituted double bond [δ_C 147.9 (C, C-7') and 118.4 (C, C-8')].

Table 1. ^{1}H-NMR (400 MHz) and ^{13}C-NMR (100 MHz) spectral data for compounds **1-3**

	1[a]		**2**[b]		**3**[a]	
Position	δ_H	δ_C	δ_H	δ_C	δ_H	δ_C
1		12.2		130.6		129.8
2		129.5		132.0		129.1
3	6.52	110.0	6.47, s	110.0	6.54, s	110.2
4		150.1		150.5		150.0
5		147.5		148.4		147.9
6	7.2	104.8	6.91, s	105.8	6.83, d (1.2)	105.1
7	4.89(d, 14)	74.2	6.17, dd (14, 1.2)	75.2	6.31, d (13.2)	74.6
8	3.37, dt (14, 8.4)	43.9	3.48, dt (14.0, 8.8)	42.2	3.64, dt (14.0, 8.8)	41.7
9a	4.76, dd (9.2, 9)	70.1	4.62, t (8.8)	70.0	4.63, t (8.8)	69.6
9b	4.26, dd (9.6, 8.4)		4.22, t (8.8)		4.33, t (8.8)	
1'		129.1		130.5		131.2
2'	6.52, s	110.0	6.44, s	109.6	6.54, s	110.3
3'		153.0		153.7		153.1
4'		135.7		139.5		138.8
5'		153.0		154.0		153.1
6'	6.52, s	110.0	6.44, s	109.6	6.54, s	110.3
7'		147.9		147.2		147.7
8'		118.4		119.7		118.0
9'		168.0		167.7		167.7
O-CH_2-O	5.991, d (0.8) 5.998, d (0.8)	102.0	6.05, d (0.8)	103.1	5.99, d(1.2)	102.1
C-3'-OMe	3.75, s	58.6	3.79	56.6	3.85, s	56.5
C-4'-OMe	3.92, s	61.2	3.70	60.7	3.92, s	61.2
C-5'-OMe	3.75, s	58.6	3.79	56.6	3.85, s	56.5
$\underline{CH_3}CO$			2.3, s	21.0		
$CH_3\underline{CO}$				171.5		
C-1"						127.1
C-2"					7.51, d (8.8)	130.6
C-3"					6.88, d (8.8)	116.3
C-4"						158.5
C-5"					6.88, d (8.8)	116.3
C-6"					7.51, d (8.8)	130.6
C-7"					7.8, d (15.6)	146.8
C-8"					6.47, d (15.6)	114.2
C-9"						167.1

[a]NMR of compounds **1** and **2** were on $CDCl_3$-$DMSOd_6$, [b]NMR of compound **3** was on $CDCl_3$
Chemical shift values were in ppm and *J* values (in Hz) were presented in parentheses.
The assignments were based on HSQC, HMBC and 1H–1H TOCSY experiments.

In addition, the absorption bands at λ_{max} 247 (1.89) and 345 (0.77) nm in the UV spectrum accounted for the dihydronaphtalene skeleton.[13]

In the HMBC of compound **1** (Figure 2), the aromatic proton at δ_H 6.52 and two methoxy proton signals (δ_H 3.92 and 3.75) showed correlations with carbon resonances at δ_C 135.7 and 153.0 indicating the presence of methoxy groups at C-3', C-4' and C-5'. The methoxy groups at δ_H 3.75 (6H) were located at C-3' and C-5', while the methoxy group at δ_H 3.92 (3H) was placed on C-4' because the correlations observed between those protons and the carbon resonances at δ_C 153.0 (C-3' and C-5') and δ_C 135.7 (C-4'), respectively. The position of the hydroxyl group at C-7 was confirmed by the HMBC correlations δ_H 7.2 (H-6)/δ_C 74.2(C-7) and δ_H 4.76 and 4.26 (H-9)/δ_C 74.2 (C-7). Furthermore, the tetrasubstituted double bond was placed on C-7'/C-8' basing on the correlations δ_H 3.37 (H-8)/δ_C 147.8 (C-7'), δ_H 4.76 (H-9)/δ_C 118.4 (C-8'), and δ_H 6.52 (H-3)/δ_C 147.9 (C-7') (Figure 1). The great coupling value (J = 14.0 Hz) between H-7 and H-8 was consistent with a *trans* diaxial relationship between these protons. The CD spectrum of compound **1** showed a positive Cotton effect at Δε 358 (1.68) nm, and a negative one at Δε 251 (–3.49) nm, suggesting an 8*R* configuration.[14] This is supported also by the fact that the other aryltetralin lignans (**4**-**6**), isolated in this work, have the 7*R*, 8*R* configuration. Based on these findings, the structure of this compound was determined to be (7*R*, 8*R*)-7',8'-dehydro-podophyllotoxin (**1**), a new natural product.

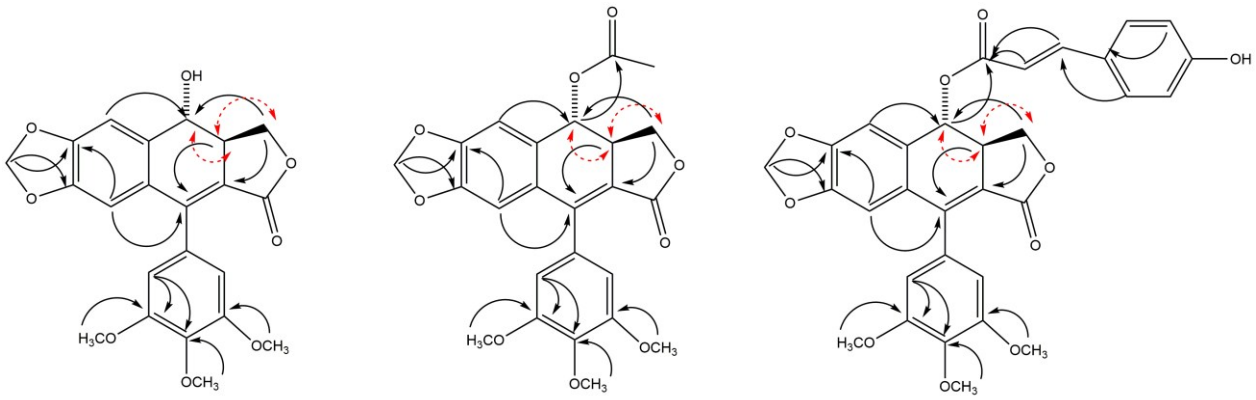

Figure 2. Selected HMBC (H→C) and COSY (H→H) correlations of compounds **1**-**3**

Compounds **2** and **3** were obtained as amorphous powders. Their HRFABMS spectra showed quasimolecular ion peaks at *m/z* 455.1324 $[M + H]^+$ ($C_{24}H_{23}O_9$) for **2**, and at *m/z* 559.1586 $[M + H]^+$ ($C_{31}H_{27}O_{10}$) for **3**, respectively. Analysis of the NMR data (Table 1) indicated that **2** and **3** share many structural features with 7',8'-dehydropodophyllotoxin (**1**). The only significant differences between the NMR spectra were the presence of an additional acetate group in **2**, and a *trans*-*p*-cumaroate group in **3**. This was evidenced by the downfield shift of the oxymethine proton H-7 at δ_H 6.17 (dd, *J* = 14.0, 1.2 Hz) in **2**, and at δ_H 6.31 (d, *J* = 13.2 Hz) in **3**. This signal appears in **1** at δ_H 4.89 (1H, d, *J* = 14.0 Hz), indicating that an acyl substitution occurred at C-7 in **2** and **3**. The presence of a methyl signal at δ_H 2.3 (3H, s), in the ^{1}H NMR spectra and acetate carbon signals at δ_C 171.5, and 21.0 in the ^{13}C NMR spectra of **2** supported this assumption. In addition, signals due to an A_2B_2 system [δ_H 7.51 (1H, d, *J* = 8.8, Hz), 6.88 (1H, d, *J* = *8*.8 Hz)] corresponding to a 1,4-disubstituted aromatic ring, and one *trans*-double bond at δ_H 7.8 (1H, d, *J* = 15.6 Hz), and 6.47 (1H, d, *J* = 15.6 Hz) were also revealed in compound **3**, indicating the presence of a an additional *trans*-*p*-coumaroyl group with respect to **1**.

Detailed analysis of the 1D and 2D NMR data of **2** and **3** enabled the assignment of all ^{1}H and ^{13}C NMR signals. ^{1}H-^{1}H COSY spectrum confirmed the presence of the aliphatic spin system formed by the protons H-9/H-8/ H-7 in both compounds (Figure 1). HMBC correlations between H-7 and C-1", and H-6 and C-7, allowed us to put the ester group at C-7, and correlations between H-8/C-7', H-7/C-8', and H-9/C-8' confirmed the dihydronaphtalene skeleton (Figure 2). In addition, the absorption bands at λ_{max} 266 (2.19) and 348 (1.61) nm in the UV spectrum of compound **2** are in accordance with a dihydronaphtalene skeleton.[13]

As performed for **1**, the relative stereochemistry of **2** and **3** was also determined by the analysis of *J* values obtained from the ^{1}H NMR spectrum, and the absolute configuration was determined to be 7(*R*), 8 (*R*) because of the positive Cotton effect at 354 (26.0), and the negative Cotton effect at 252 (−44.45) nm observed in the CD spectra of compound **2**. In addition, mild basic hydrolysis (Na_2CO_3:MeOH:H_2O) of **2** and **3** separately, afforded **1**, identical in all aspects with the natural product, confirming their identity. Based on these findings, the structure of these compounds was determined to be (7*R*, 8*R*)-7′,8′-dehydro acetyl podophyllotoxin (**2**), and (7*R*, 8*R*)-7′,8′-dehydro *trans*-*p*-cumaroyl podophyllotoxin (**3**), which represent new natural products.

The chemical structures of the known compounds were identified as podophyllotoxin (**4**),[7] acetylpodophyllotoxin (**5**),[7] 5'-desmethoxy-β-peltatin A methylether (**6**),[7] acetylpicropodophyllotoxin (**7**),[15] burseranin (**8**),[7] hinokinin (**9**),[16] and the coumarin scopoletin (**10**),[17] by comparison of the physicochemical and spectroscopic data (IR, MS, 1D and 2D NMR) with that reported in the literature.

Podophyllotoxin (**4**), acetylpodophyllotoxin (**5**), 5'-desmethoxy-β-peltatinA methylether (**6**), and burseranin (**8**) were previously isolated from this plant species, and their cytotoxic activity has been described.[7] Furthermore, *in vivo* effects over cell cycle, cell migration and microtubules on zebrafish embryos demonstrated that these natural lignans act by disturbing tubulin.[8] Acetylpicropodophyllotoxin (**7**) was a constituent of *Hernandia ovigera* and it is a potent, selective inhibitor of type I insulin-like growth factor receptor (IGF-IR).[18] Its desacetyl derivative, is currently used with notable success in clinical trials that include patients with aggressive types of epithelial tumors.[19] Hinokinin (**9**) has been isolated from several plant species and its cytotoxic activity against several cell lines has been documented.[20] Scopoletin (**10**) has been isolated from several plant species, this coumarin induce cell cycle arrest and increase

apoptosis in human prostate tumor cells and human leukemia cell line via activation of caspase-3.[21]

Evaluation of the cytotoxic activity of compounds **1-3** against the cancer cell lines KB, PC-3, MCF-7, and HF-6 showed that all of them displayed good activity against KB, PC-3 and HF-6, but were not active against the MCF-7 cell line (Table 2). When compared with podophyllotoxin (**4**) (ED_{50} =2.10×10^{-4} μM), compounds **1** and **3** were most active against PC-3 cell line displaying similar toxicity (ED_{50} = 2.4×10^{-5} and 2.42×10^{-5} μM, respectively), while compound **2** was the less active one (ED_{50} = 0.06 μM). Lignans **1-3** showed moderate activity against KB and HF-6 cell lines when compared to **4**.

Table 2. IC_{50} values (μM) of compounds **1-3** isolated from *B. fagaroides*.

Compound	KB	PC-3	MCF-7	HF-6
1	0.25 ± 0.0025	2.42×10^{-5} ± 0.004	> 9.7	0.012 ± 0.008
2	0.297 ± 0.0006	0.061 ± 0.0089	> 8.8	0.066 ± 0.055
3	3.61 ± 0.08	2.42×10^{-5}±0.0036	> 7.2	1.27 ± 0.027
Camptothecin	4.54×10^{-3} ± 0.009	2.758 ± 0.006	3.67×10^{-4} ± 0.015	1.58×10^{-5}± 0.007
Podophyllotoxin	2.10×10^{-4} ± 0.003	2.05 ± 0.009	2.30×10^{-4}± 0.005	0.018 ± 0.05

KB: nasopharyngeal cancer, PC-3: prostate cancer, MCF-7: breast cancer, HF-6: colon cancer

In order to measure the effect of natural lignans **1-3** over cell cycle and morphology on the zebrafish (*Danio rerio*) model, we used the serine 10-phosphorylated modification of histone H3 (H3S10ph) as a mitotic marker detected by indirect immunofluorescence on whole zebrafish embryos as described previously.[8] Natural lignans (**1-3**) were assayed at a standard concentration of 10 μg/mL in whole embryos. Nocodazole and aphidicolin were used as controls at the same concentration. Figure 3 shows the effect over the number of marked nuclei (H3S10ph) on the treated embryos, and the quantification of the fold change is presented in Figure 4. The results indicated that embryos treated with the natural lignans **1-3** showed a marked increase on

H3S10ph positive nuclei by 1.92, 2.41 and 2.57 times, respectively, with respect to the control (DMSO).

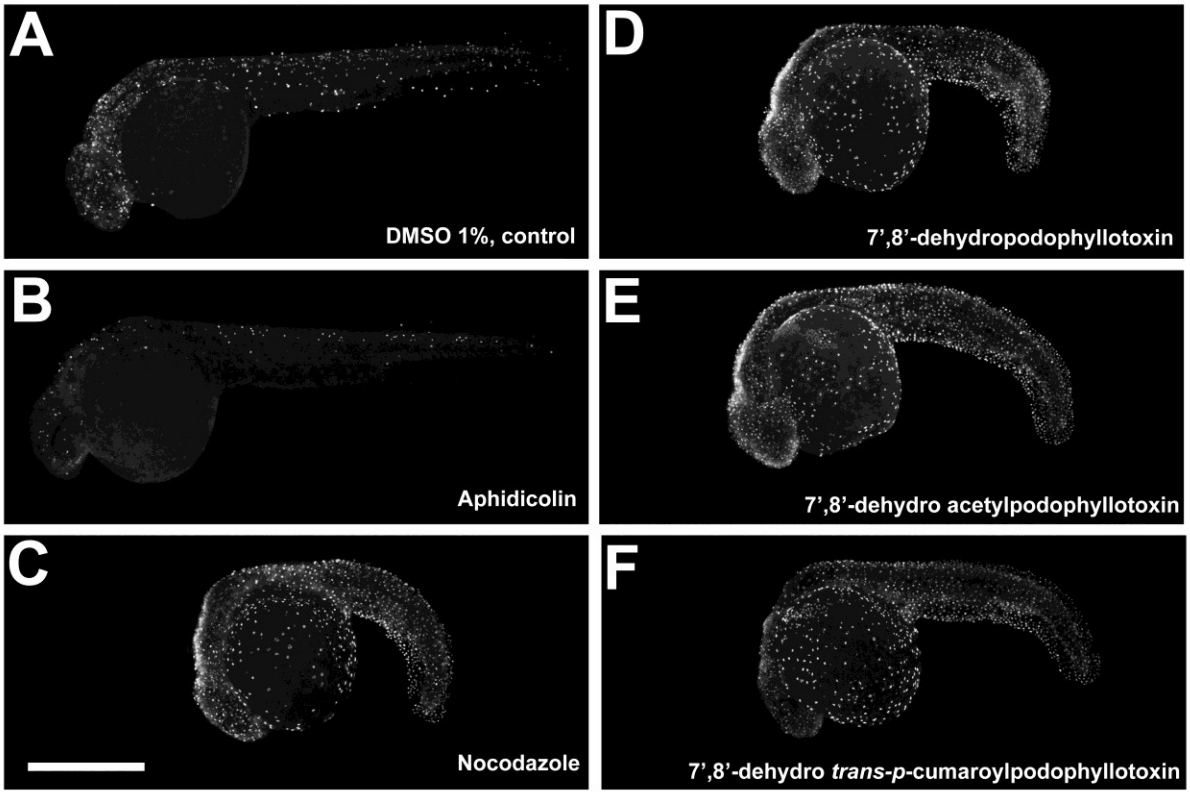

Figure 3. Histone H3 phosphorylated at serine 10 (H3S10ph) whole mount fluorescence immunolocalization in 30 h post fertilization (hpf) zebrafish embryos. 24 hpf embryos were treated for 6 h with corresponding compounds and afterwards were immunostained against the mitotic marker H3S10ph. Embryos were imaged by conventional fluorescence microscopy. A, Dimethyl sulfoxide 1% (Control). B, Aphidicolin. C, Nocodazole. D, 7',8'-dehydropodophyllotoxin (**1**). E, 7',8'-dehydro acetyl podophyllotoxin (**2**). F, 7',8'-dehydro-*trans*-p-coumaroyl podophyllotoxin (**3**). Scale bar, 500 μm.

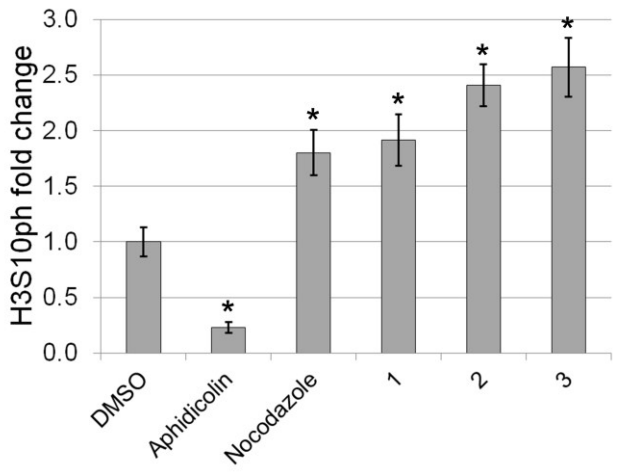

Figure 4. Results of H3S10ph-based evaluation of the cell-cycle effect of natural lignans **1-3** using zebrafish embryos. The fold changes were determined using the values for treated embryos and compared against the control treated embryos. * Significant differences (p<0.01). These results are also presented in supplementary material Table 1.

Also, these compounds caused morphological changes of the embryos modifying the circularity by 0.78, 0.73 and 0.77, respectively (Figure 5), with respect to the embryos treated with the vehicle. This effect was observed previously for those compounds that interfere with the stability of microtubules, as podophyllotoxin.[8] These results indicated that compounds **1-3** promote mitotic arrest and induction of morphological changes by a similar manner to that of the antimitotic drugs nocodazole and podophyllotoxin.

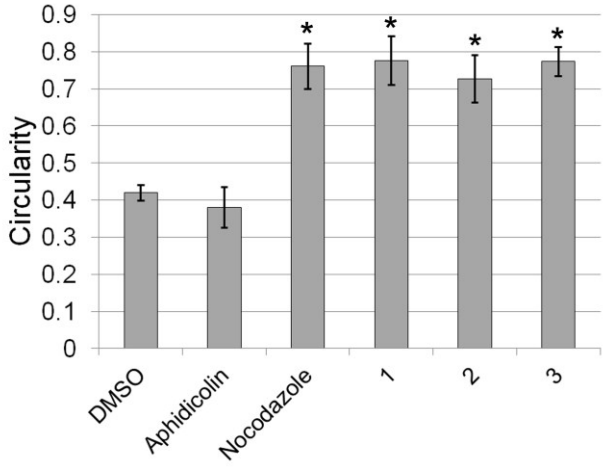

Figure 5. Morphological effect of pure compounds of *B. fagaroides* var. *fagaroides* evaluated by measuring the circularity of zebrafish embryos. * Significant difference in circularity values (p<0.01). These results are also presented in supplementary material Table 2.

Epiboly migration on zebrafish embryos has been used to screen compounds that destabilize microtubules.[22] By using this approach, we analyzed the effect of the pure lignans (**1-3**) on epiboly migration in zebrafish embryos. Embryo treatment started at sphere stage and afterwards all treatment groups were fixed at the same time point when the control DMSO treated embryos reached 90% of epiboly. As shown in Figure 6, compounds **1-3** induced epiboly delay and larger blastoderm cells and nuclei as evidenced by phalloidin alexa and SYTOX green staining of the embryos. These effects show similarities to the treatment with nocodazol, which caused more penetrant phenotype. In contrast, embryos treated only with vehicle or aphidicolin, showed normal epiboly migration movement since the yolk is fully covered. This result suggested that treatment of the embryos with compounds **1-3** affected microtubule cytoskeleton.

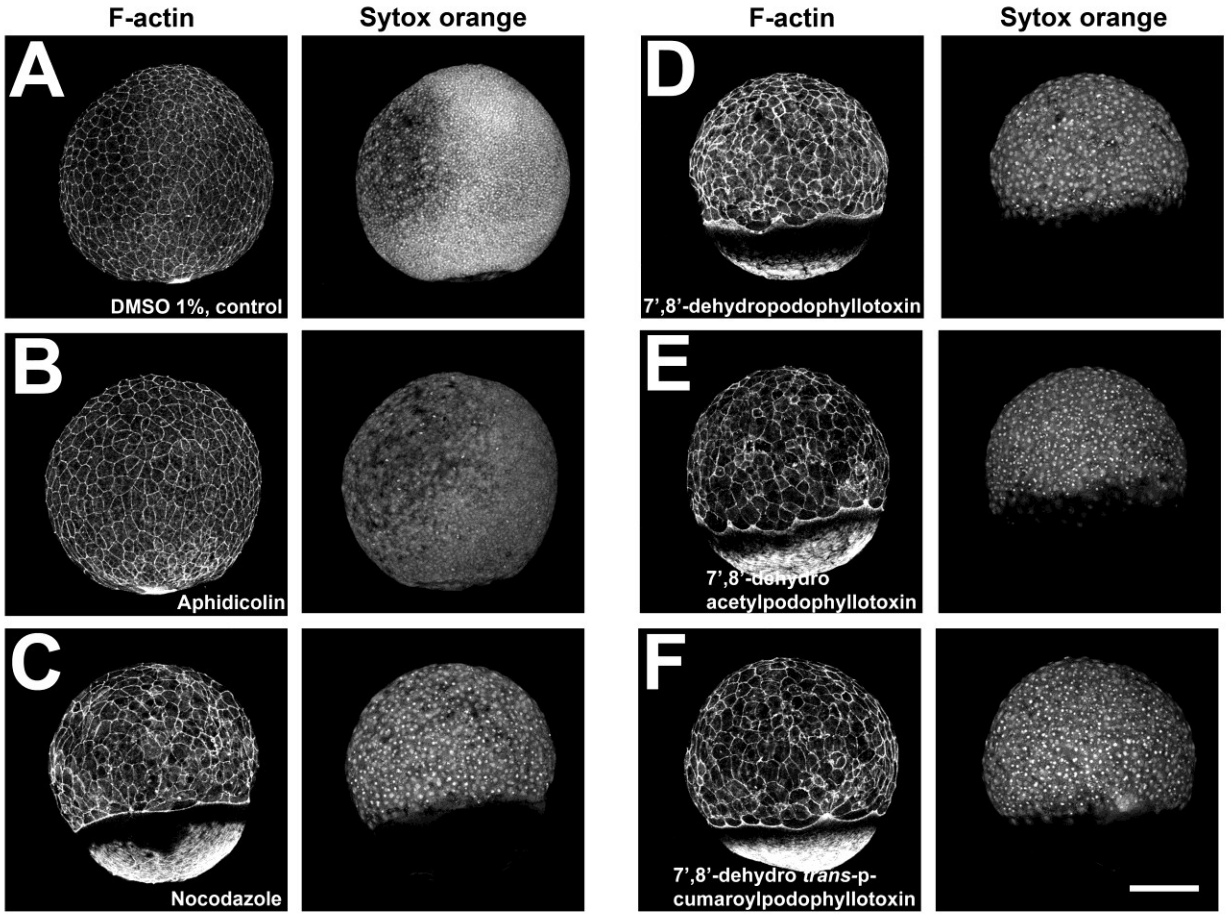

Figure 6. Whole mount localization of actin filaments and nuclei in zebrafish embryos after treatment with compounds **1**-**3** to determine their effect on cell migration. Sphere stage zebrafish embryos were treated with different compounds until control embryos reached 90% epiboly, fixed and processed for actin and nuclei staining and visualized by confocal microscopy. A, Dimethyl sulfoxide (Control). B, Aphidicolin. C, Nocodazole. D, 7',8'-dehydropodophyllotoxin (**1**). E, 7',8'-dehydro acetyl podophyllotoxin (**2**). F, 7',8'-dehydro-*trans*-p-coumaroyl podophyllotoxin (**3**). Scale bar, 250 μm.

In order to corroborate that lignans **1-3** effectively act directly over the microtubule cytoskeleton, we performed a tubulin immunolocalization on zebrafish embryos. For this assay, embryos were treated with the pure lignans (**1-3**) starting at sphere stage and embryos of all treatment groups were fixed when they reached 50% of epiboly, therefore they were stage matched. This stage was chosen since the yolk cell present large and conspicuous microtubules that are readily visualized by confocal microscopy as previously reported.[8] Figure 7 shows embryos treated with each of the pure lignans **1**-**3** at a concentration of 200 μg/mL. It is notable the absence of microtubule array

in the embryos treated with lignans **1**-**3**, in comparison with the control (DMSO 1%) and aphidicolin treatments, which indicate that these compounds promote destabilization of the microtubules. This effect is comparable to that observed by the nocodazole treatment. This result confirms that the *in vitro* cytotoxic activity, as well as the *in vivo* effects over cell cycle and morphological changes observed for these three natural lignans is due to their effect over microtubules.

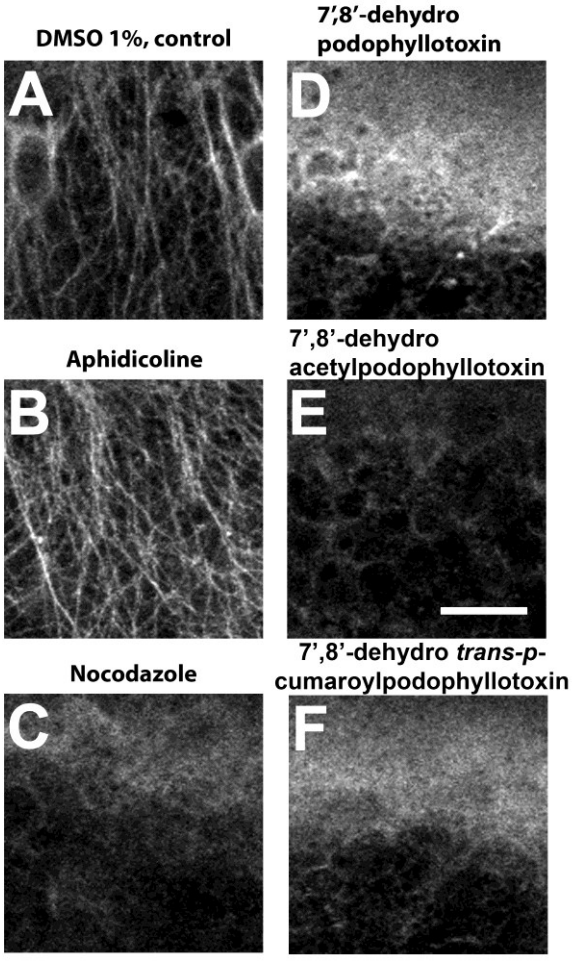

Figure 7. Whole mount immunolocalization of yolk cell microtubules in zebrafish embryos after treatment with *B. fagaroides* compounds. Sphere stage zebrafish embryos were treated with different compounds until all treatment groups embryos reached 50% epiboly fixed and processed for microtubule fluorescent immunolocalization and visualized by confocal microscopy. A, Dimethyl sulfoxide (Control). B, Aphidicolin. C, Nocodazole. D, 7',8'-dehydropodophyllotoxin (**1**). E, 7',8'-dehydro acetyl podophyllotoxin (**2**). F, 7',8'-dehydro-*trans*-*p*-coumaroyl podophyllotoxin (**3**). Scale bar, 25 μm.

3. Conclusions

Three new aryldihydronaphthalene-type lignans (**1**-**3**) were isolated from the stem bark of *Bursera fagaroides*, along with six known podophyllotoxin-type lignans (**4**-**9**) and one coumarin (**10**). Compounds **1**-**3** were identified for the first time in the genus *Bursera*. Compounds **1**-**3** showed marked cytotoxic activity against human nasopharyngeal (KB), colon (HF-6) and prostate (PC-3) cancer cell lines. Evaluation of the effect of compounds **1**-**3** over the developing zebrafish embryo model, showed that these compounds promote mitotic arrest and a delay in cell migration by disturbing microtubule cytoskeleton. This *in vivo* activity suggest that these natural lignans affect tubulin by a similar manner as that of podophyllotoxin.

4. Experimental section

General procedures

NMR spectra were acquired on a Varian Unity NMR spectrometer operating at 400 MHz for ^{1}H and 100 MHz for ^{13}C nuclei. Chemical shifts are listed in parts per million (ppm), referenced to $CDCl_3$ and were made on the basis of ^{1}H-^{1}H gCOSY, NOESY, gHSQC and gHMBC spectral analysis as required. NMR experiments performed in $CDCl_3$ are referenced to Me_4Si (0 ppm). FABMS spectra in a matrix of *m*-nitrobenzyl alcohol or glycerol were recorded on a JEOL JMX-AX 505 HA mass spectrometer. All reagents and solvents used were analytical grade. Optical rotations were acquired with a Perkin-Elmer 241MC polarimeter (10 cm, 1 mL cell) at the

sodium D line. IR spectra on a Vectro 22, Bruker spectrometer, and UV spectra on an Agilent 8453 (1 cm, 3 mm cell) spectrometer. CD spectra were recorded on a CD spectropolarimeter (model J-715, Jasco Analytical Instruments) using a 0.1-cm path length cell over the 190–260-nm range. The purity of lignans was checked by reverse-phase HPLC, using an Agilent Infinity 1260, equipped with autosampler, photodiode array detector, a quaternary pump and an Agilent C-P18 column (2.7 μm, 4.6 X 50 mm) with MeOH-H_2O (1:1) as isocratic eluent system, UV detection at 215 nm and a flow rate of 1 mL/min.: 7', 8' dehydro-podophyllotoxin (**1**) (t_R = 0.93 min), 7', 8' dehydro-acetylpodophyllotoxin (**2**, t_R = 1.80 min), podophyllotoxin (**4**, t_R = 0.87 min), acetyl podophyllotoxin (**5**, t_R = 1.62 min), 5'-desmethoxy-β-peltatin-A-methylether (**6**, t_R = 1.97 min), acetyl picropodophyllotoxin (**7**, t_R = 2.45 min), Burseranin (**8**, t_R = 2.29 min), hinokinin (**9**, t_R = 1.38 min).

Plant material

The bark of *B. fagaroides* var. *fagaroides* (H.B.K.) Engl. was collected in the village of Capula between Zacapu and Quiroga, Michoacán, México. Its identification was made at the Herbarium of the Instituto Mexicano del Seguro Social (registration number-12 051 IMSSM) and at the Institute of Botany, University of Guadalajara (IBUG-140 748), México.

Extraction and isolation

The stem bark of *Bursera fagaroides* var. *fagaroides* (1.140 g) was extracted by maceration at room temperature thrice with CH_2Cl_2, (3L) and was concentrated to dryness under reduced pressure. The three extracts were combined (33 g) and fractionated by column chromatography

on 990 g of silica gel (70-230 mesh) eluting with *n*-hexane-EtOAc mixtures of increasing polarity to yield five fractions: F-1 (1.2 g, 100:00 to 9:1), F-2 (2.72 g, 4:1), F-3 (5.1 g, 4:1), F-4 (8.9 g, 7:3), F-5 (1.6 g, 1:1).

F-2 was subjected to CC (90:10→70:30, n-hexane/CH_2Cl_2), A total of 46 fractions were collected, each of about 50 mL. Similar fractions were combined according to their TLC properties to yield two main subfractions. Fractions eluted with *n*-hexane-CH_2Cl_2 (9:1) were chromatographed on silica gel to yield 131 mg of β-sitosterol and 36.5 mg of burseranin (**8**). Fractions eluted with n-hexane-CH_2Cl_2 (8:2) were combined and the residue (1.21 g) was purified by column chromatography (90:10→00:100, n-hexane/EtOAc) to afford 278.5 mg of acetylpodophyllotoxin (**5**), 36.5 mg of burseranin (**8**) and 145 mg of 7',8'-dehydro-acetylpodophyllotoxin (**2**).

F-3 was chromatographed on silica gel column (9:1 → 7:3) *n*-hexane/EtOAc. Fractionation gave rise to three fractions. The subfraction F-3-2 (649.3 mg), eluted with 8:2, was then purified by preparative TLC eluted with 95:05 benzene-EtOAc, to yield 28.4 mg of hinokinin (**9**) and 48.3 mg of burseranin (**8**). The subtraction F-3-3, eluted with 7:3 *n*-hexane-EtOAc (2.8 g) was purified by column chromatography of silica gel, eluting with a gradient of *n*-hexane/CH_2Cl_2 (8:2 → 6:4) to yield 117 mg of 5'-desmethoxi β-peltatin A methyl ether (**6**), and 15 mg of acetylpicropodophyllotoxin (**7**).

F-4 was subjected to CC eluted with an isocratic mixture of 65:35 *n*-hexane/EtOAc, obtaining 85 fractions of 100 mL each. Fractions 20-36 were a mixture of two lignans, determinated by NMR spectra. This mixture was purified by semi preparative RP HPLC eluting with CH_3OH-H_2O (52:48) obtaining 254 mg of 5'-desmethoxy-β-peltatin-A-methyl-ether (**6**, t_R = 1.97 min) and 40.5

mg of 7',8'-dehydro-acetyl-podophyllotoxin (**2**, t_R = 1.80 min). The yields were based on peak areas of the HPLC chromatogram.

Fractions 40-65 were combined and the residue (1.6 g) was adsorbed on reverse phase silica gel and subjected to RP column chromatography eluted with a gradient of MeOH:H_2O (1:1→6:4) to yield 39 fractions of 50 mL each, which were combined in three main fractions: F4-1 (42 mg, 50:50), F4-2 (185 mg, 55:45), and F4-3 (290 mg). Fraction F4-1 was constituted mainly by one compound which was purified by crystallization from acetone to yield 8 mg of scopoletin (**10**). F4-2 was purified by column chromatography of silica gel eluting with an isocratic mixture of *n*-hexane/EtOAc (6:4), to give two main fractions. The less polar fraction was purified by preparative RPTLC eluted with CH_3CN-H_2O (72:25) to yield 13 mg of 7',8'-dehydro *trans*-*p*-coumaroylpodophyllotoxin (**3**). The most polar fraction was purified by preparative TLC eluted with benzene/EtOAc (55:45) (three developments) to afford 8 mg of podophyllotoxin (**4**) and 42 mg of 7',8'-dehydropodophyllotoxin (**1**).

7´, 8´-dehydro-podophyllotoxin (1). White amorphous powder, mp 271-273 °C; purity = 98%; $[\alpha]^{24}_D$ –95° (c 0.090, $CHCl_3$); UV ($CHCl_3$) λ_{max}, nm (log ε): 247 (1.89), 345 (0.77); CD (c 1.33 × 10^{-4} M, $CHCl_3$) nm (Δε): 3.58 (1.68), 314 (0.166), 278 (0.438), 251 (-3.49); IR (KBr) υ_{max} cm^{-1}: 3440.9, 2921.6, 1757.5, 1608.6, 1503.3, 1480.5, 1331.6, 1280.9, 1161.3 cm^{-1}; ^{1}H-NMR (400 MHz, $CDCl_3$-$DMSOd_6$) and ^{13}C NMR (100 MHz, $CDCl_3$-$DMSOd_6$) data see Table 1. FABHRMS *m/z* 413.1301 $[M + H]^+$ (calcd for $C_{22}H_{21}O_8$, $[M + H]^+$ 413.1191).

7´, 8´-dehydro-acetylpodophyllotoxin (2). White amorphous powder, mp 262-264 °C; purity = 95%; $[\alpha]^{24}_D$ –87° (c 0.015, $CHCl_3$); UV ($CHCl_3$) λ_{max}, nm (logε): 266 (2.19), 287 (0.472), 348 (1.61); CD (*c* 1.33 × 10^{-4} M, $CHCl_3$) λ_{max}(Δε): 354(26.0), 313 (4.65), 280 (6.08), 252 (-44.45) nm; IR (KBr) υ_{max} cm^{-1}: 2921.1, 2848.9, 1757.8, 1608.2, 1516.2, 1480.5, 1349.6, 1280.9, 1129.4

cm^{-1}; ^{1}H-NMR (400 MHz, $CDCl_3$-$DMSOd_6$) and ^{13}C NMR (100 MHz, $CDCl_3$-$DMSOd_6$) data see Table 1. FABHRMS m/z 455.1324 $[M + H]^+$ (calcd for $C_{24}H_{23}O_9$ $[M + H]^+$ 455.1342).

7´, 8´-dehydro-*trans*-*p*-coumaroylpodophyllotoxin (3). White amorphous powder, mp 287-288 °C; purity = 95%; $[\alpha]^{24}_D$ –75.0° (c 0.014, $CHCl_3$); IR (KBr) υ_{max} cm^{-1}: 2920.2, 1757.2, 1608.6, 1503.6, 1483.6, 1330.9, 1280.6, 1161.1 cm^{-1}; ^{1}H-NMR (400 MHz, $CDCl_3$) and ^{13}C NMR (100 MHz, $CDCl_3$) data see Table 1. FABHRMS m/z 559.1586 $[M + H]^+$ (calcd for $C_{31}H_{27}O_{10}$ $[M + H]^+$ 559.1604).

Basic hydrolysis of 2 and 3.

A quantity of 7 mg of **2** and 4.2 mg of **3** were separately dissolved in a solution of 7:3:1 THF, MeOH, H_2O and then stirred up with a solution 10% K_2CO_3 (2 equiv) for 9 hours at room temperature. The product was purified by preparative TLC eluted with 1:1 Hexane-EtOAc to yield 2 mg and 0.75 mg respectively of compound **1**.

Cytotoxicity assay

The *in vitro* cytotoxicity was determined by the sulphorhodamine B (SRB) (MP Biomedicals, LLC) protein staining assay[23,24] using KB (nasopharyngeal), HF-6 (colon), MCF-7 (breast), and PC-3 (prostate) cancer cell lines. The cell cultures were maintained in RPMI-1640 medium supplemented with 10% fetal bovine serum, 5000 units/mL penicillin, 5 mg/mL streptomycin, 7.5% $NaHCO_3$, and cultured in a 96-well microtiter plate (10^4 cells/mL, 190 μl/well) at 37 °C in a 5% CO_2-air atmosphere (100% humidity). The cells at the log phase of growth were treated in triplicate (n=3) with different concentrations of the test compounds (0.16, 0.8, 4 and 20 μg/mL),

and incubated for 72 h. The cell concentration was determined by protein analysis. The optical density was measured at 590 nm with an ELISA-Reader (Molecular Devices, SPECTRA max plus 384). Results were expressed as the concentration that inhibits 50% of control growth after the incubation period (IC_{50}). The values were estimated from a semi-log plot of the extract concentration (μg/mL) against the percentage of viable cells. Camptothecin and podophyllotoxin were included as positive standards. Pure products with $ED_{50} \leq 4$ μg/mL were considered active according to the National Cancer Institute (NCI) guidelines described in the literature.[25]

Statistical analysis

The results were analyzed using one-way ANOVA followed by Kaplan-Meier estimation of survival and Cox´s regression through the statistical package SPSS V.15.

Fish maintenance and strains

Wild type zebrafish (*Danio rerio*) were obtained from natural crosses and raised at 28°C. Embryo stages were determined by morphological criteria according to Kimmel and collaborators.[26] Zebrafish were handled in compliance with the local animal welfare regulations EU Directive 2010/63/EU indications[27] and approved by Comité de ética (Instituto de Biotecnología, UNAM).

Chemical treatment of Zebrafish embryos

Treatments were performed as previously described.[8] In brief, compounds for chemical treatments were diluted in anhydrous DMSO (276855, Sigma-Aldrich). Plant extracts for

screening were tested at a standard final concentration of 200 μg/mL in the water. Control compounds were aphidicolin (10 μg/mL, A0781, Sigma-Aldrich) and nocodazole (10 μg/mL, M1404, Sigma-Aldrich). 10 zebrafish embryos of 24 hour post fertilization age for each treatment, were incubated at 28ºC in egg water (60 μg/mL of "Instant Ocean" sea salts in distilled water) for 6 hours in 48-well plates.[28] 3 μL of each compound stock solution was added to a total volume of 300 μL at the beginning of the incubation. Control embryos were treated with DMSO alone at 1% final concentration (v/v), and processed as described below.

Immunofluorescense

Whole-mount immunostaining in zebrafish embryos was used to determine the effect of pure compounds as previously described.[29] The primary antibody rabbit IgG anti phospho histone H3 (sc-8656-R, Santa Cruz Biotechnology) was diluted 1:100 in blocking buffer (final concentration 2 μg/mL), and as secondary antibody a goat anti-rabbit Alexa Fluor 488 (A11008, Molecular Probes) solution 1:100 in blocking buffer was used. For the analysis of cell migration embryos were stained with SYTOX orange (S11368, Molecular Probes) diluted 1:2000 in blocking buffer to visualize DNA and nuclei and counter-stained with phalloidin Alexa 488 (A12379, Molecular Probes). For tubulin immunolocalization as primary antibody a mouse anti tubulin monoclonal antibody diluted 1:500 in blocking buffer was used (T9026, Sigma-Aldrich) and a goat anti-mouse coupled to Alexa 647 (A21235, Molecular Probes) diluted 1:1000 in blocking buffer was used as a secondary antibody. Embryos were mounted in 2.5% methyl cellulose in PBS for epifluorescence or in 1% low melting point agarose for confocal microscopy visualization.

Fluorescence microscopy and image analysis

Fluorescent signal corresponding to H3S10ph positive cells in whole zebrafish embryos where imaged by fluorescence microscopy with a 5x objective 0.15 N.A. PlanNeofluoar under a Zeiss Axioscop Microscope. Image stack (10 to 14 images per embryo) were coupled into a single focused image with the public domain ImageJ software[30] with the stack focuser plugin. To quantify the phospho histone H3 positive nuclei in each embryo, focused images were made binary by thresholding to highlight in black H3S10ph positive nuclei and in white the background, and automatically quantified by the analyze particles command in ImageJ software. Embryo contour was delineated on each image and the circularity was measured in ImageJ. The Student´s t-test statistical analysis was performed in Excel.

Confocal laser scanning microscopy

Zebrafish embryos stained with the specified fluorescent dyes were visualized on a FluoView FV1000 confocal microscope coupled to an inverted IX81 Olympus microscope with a UPlanSApo 10x (numeric aperture 0.4) objective or a UPlanSApo 20x (numeric aperture 0.75) objective was used. The pinhole aperture was maintained at 200. Serial optical sections were obtained with a z-step of 8 or 2 µm. Images were processed with the public domain software ImageJ[30] and Adobe Photoshop.

Acknowledgements

Mayra Yaneth Antúnez Mojica and Mario A. Mendieta-Serrano acknowledges fellowships 253315 and 323762 respectively from CONACYT. Partial financial support from CONACYT, México (Grants 82851, 240801 and 222714), and UNAM (Grants IX201110 and IN205612) is acknowledged. The authors thank Laboratorio Nacional de Estructura de Macromoléculas

(Conacyt 251613) for the spectroscopic and mass analyses, and Confocal Microscopy Service provided by Laboratorio Nacional de Microscopía Avanzada, Instituto de Biotecnología, Universidad Nacional Autónoma de México.

Conflict of interest

The authors declare that there are no conflicts of interest

Notes

[a]Centro de Investigaciones Químicas-IICBA, and [d]Centro de Investigación en Biotecnología, Universidad Autónoma del Estado de Morelos, Avenida Universidad 1001, Chamilpa, Cuernavaca, Morelos 62209, México. [b]Facultad de Ciencias, Universidad Antonio Nariño, Armenia, Quindío, Colombia. [c]Departamento de Genética del Desarrollo y Fisiología Molecular, Instituto de Biotecnología, Universidad Nacional Autónoma de México, A.P. 510-3, Cuernavaca, Morelos 62271, México.

References

1. R. Medina-Lemus, *Flora del valle de Tehuacán-Cuicatlán*. Instituto de Biología, Universidad Nacional Autónoma de Méxi*co*, 2008, **66**, 1-76.
2. R. L. Huacuja, N. M. Delgado, L. A. Carranco, L. R. Reyes, G. A. Rosado, *Arch. Invest. Med. (Mex)* 1990, **21**, 393–398.
3. P. Rosas-Arreguin, P. Arteaga-Nieto, R. Reynoso-Orozco, J. C. Villagomez-Castro, M. Sabanero-Lopez, A. M. Puebla-Perez, C. Calvo-Mendez, *Exp. Parasitol.* 2008, **119**, 398–402.

4. A. M. Puebla-Pérez, L. Huacuja, G. Rodríguez, X. Lozoya, G. Zaitseva-Petrovna, M. Villaseñor-García, *Phytother. Res.* 1998, **12**, 545–548.
5. E. Bianchi, K. Sheth, J. R. Cole, *Tetrahedron Lett*. 1969, **10**, 2759–2762.
6. R. Velazquez-Jimenez, J. M. Torres-Valencia, C. M. Cerda-Garcia-Rojas, J. D. Hernandez-Hernandez, L. U. Roman-Marin, J. J. Manriquez-Torres, M. A. Gomez-Hurtado, A. Valdez-Calderon, V. Motilva, S. Garcia-Maurino, *Phytochemistry* 2011, **72**, 2237–2243.
7. A. M. Rojas-Sepúlveda, M. Mendieta-Serrano, M. Y. Antúnez, E. Salas-Vidal, S. Marquina, M. L. Villarreal, A. M. Puebla, J. I. Delgado, L. Alvarez, *Molecules*, **17**, 9506-9519.
8. M. Y. Antúnez, A. M. Rojas-Sepúlveda, M. A. Mendieta-Serrano, L. González, S. Marquina-Bahena, E. Salas-Vidal, L. Alvarez., Submitted.
9. M. A. Leyva-Peralta, R. E. Robles-Zepeda, A. Garibay-Escobar, E. Ruiz-Bustos, L. Alvarez, J. C. Gálvez-Ruiz, *BMC Complement. Altern. Med.* 2015, **15**(13), 1–7.
10. I. Alejandre-García, L. Alvarez, A. Cardoso-Taketa, L. González-Maya, M. Antúnez, E. Salas-Vidal, F. Díaz, S. Marquina-Bahena, M. L. Villarreal, *Evid. Based Complement. Alternat. Med.*, 2015, **298463**, 11 pages.
11. J. A. Moreno-Escobar, L. Alvarez, V. Rodríguez-López, S. Marquina, *Phytochemistry Lett.*, 2013, **6**, 610-613.
12. M. Acevedo, P. Nuñez, L. Gónzález-Maya, A. Cardoso, M. L. Villarreal, *J. Clin. Toxicol.*, 2015, **5**, 232 doi:10.4172/2161-0495.1000232.
13. T. J. Schmidt, S. Vößing, M. Klaes, S. Grimme, *Planta Med.*, 2007, **73**: 1574–1580.
14. H. Otsuka, H. Kuwabara, H. Hoshiyama, *J. Nat. Prod.*, 2008, **71**, 1178-1181.

15. J.-Q. Gu, E. J. Park, S. Totura, S. Riswan, H. H. S. Fong, J. M. Pezzuto, A. D. Kinghorn, *J. Nat. Prod.* 2002, **65**, 1065-1068.

16. V. D. Gangan, S. S. Hussain, *Journal of Pharmacy Research* 2011, **4**, 4265-4267.

17. T.-S. Wu, L.-S. Shi, J.-J. Wang, S.-Ch. Iou, H.-Ch. Chang, Y.-P. Chen, Y.-H. Kuo, Y.-L. Chang, Ch.-M. Teng, *Journal of the Chinese Chemical Society*, 2003, **50**, 171-178.

18. Q. G. Jian, P. E. Jung, T. Stephan, R. Seodarsono, H. S. Harry, J. M. Pezzuto, D. A. Kinghorn, *J. Nat. Prod.* 2002, **65**,1065-1068.

19. F. Z. Zhiwei-Huang, H. Zhen, L. Zhou, H. M. Amin, P. Shi, *Leukemia & Lymphoma*, 2014, **55**, 1876-1883.

20. M. C. Marcotullio, A. Pelosi, M. Curini, *Molecules* 2014, **19**, 14862-14878.

21. W. Liu, J. Hua, J. Zhou, H. Zhang, H. Zhu, Y. Cheng, R. Gust, *Med. Chem. Lett.* 2012, **22**, 5008-5012.

22. H. S. Moon, E. M. Jacobson, S. M. Khersonsky, M. R. Luzung, D. P. Walsh, W. Xiong, J. W. Lee, P. B. Parikh, J. C. Lam, T. W. Kang, G. R. Rosania, A. F. Schier, Y. T. Chang, *J. Am. Chem. Soc.* 2002, **124**, 11608-11609.

23. P. Houghton, R. Fang, I. Techatanawat, G. Steventon, P. J. Hylands, C. C. Lee, *Methods* 2007**, 42**, 377-387.

24. P. Shekan, R. Storeng, D. scudiero, A. Monks, J. McMahon, D. Vistica, J. T. Warren, H. Bokesch, S. Kenney, M. R. Boyd, *J. Natl. Cancer Instit.*, 1990, **82**, 1107-1112.

25. M. Suffness, J. M. Pezzuto, *Assays related to cancer drug discovery*. Academic Press: London, 1991, **6**, 71-133.

26. C. B. Kimmel, W. W. Ballard, S. R. Kimmel, B. Ullmann, T. F. Schilling, *Dev Dyn* 1995**, 203**, 253-310.

27. U. Strahle, S. Scholz, R. Geisler, P. Greiner, H. Hollert, S. Rastegar, A. Schumacher, I. Selderslaghs, C. Weiss, H. Witters, T. Braunbeck, *Reprod Toxicol*, 2012, **33**, 128-132.

28. M. Westerfield, *The zebrafish book. A guide for the laboratory use of zebrafish (Danio rerio)*. 4th ed. ed.; Univ. of Oregon Press: Eugene, 2000.

29. M. A. Mendieta-Serrano, D. Schnabel-Peraza, H. Lomelí, E. Salas-Vidal, *Gene Expression Patterns*. In press.

30. M. D. Abramoff, P. J. Magelhaes, S. J. Ram, *Biophotonics International*, 2004, **11**, 36-42.

Figure legends

Figure 1. Structures of **1**-**10** from the stem bark of *B. fagaroides*

Figure 2. Selected HMBC (H→C) and COSY (H→H) correlations of compounds **1**-**3**

Figure 3. Histone H3 phosphorylated at serine 10 (H3S10ph) whole mount fluorescence immunolocalization in 30 h post fertilization (hpf) zebrafish embryos. 24 hpf embryos were treated for 6 h with corresponding compounds and afterwards were immunostained against the mitotic marker H3S10ph. Embryos were imaged by conventional fluorescence microscopy. A, Dimethyl sulfoxide 1% (Control). B, Aphidicolin. C, Nocodazole. D, 7',8'-dehydropodophyllotoxin (**1**). E, 7',8'-dehydro acetyl podophyllotoxin (**2**). F, 7',8'-dehydro-*trans*-p-coumaroyl podophyllotoxin (**3**). Scale bar, 500 μm.

Figure 4. Results of H3S10ph-based evaluation of the cell-cycle effect of natural lignans **1**-**3**

Figure 5. Morphological effect of pure compounds of *B. fagaroides* var. *fagaroides* evaluated by measuring the circularity of zebrafish embryos. * Significant difference in circularity values (p<0.01). These results are also presented in supplementary material Table 2.

Figure 6. Whole mount localization of actin filaments and nuclei in zebrafish embryos after treatment with compounds **1**-**3** to determine their effect on cell migration. Sphere stage zebrafish

embryos were treated with different compounds until control embryos reached 90% epiboly, fixed and processed for actin and nuclei staining and visualized by confocal microscopy. A, Dimethyl sulfoxide (Control). B, Aphidicolin. C, Nocodazole. D, 7',8'-dehydropodophyllotoxin (**1**). E, 7',8'-dehydro acetyl podophyllotoxin (**2**). F, 7',8'-dehydro-*trans*-p-coumaroyl podophyllotoxin (**3**). Scale bar, 250 μm.

Figure 7. Whole mount immunolocalization of yolk cell microtubules in zebrafish embryos after treatment with *B. fagaroides* compounds. Sphere stage zebrafish embryos were treated with different compounds until all treatment groups embryos reached 50% epiboly fixed and processed for microtubule fluorescent immunolocalization and visualized by confocal microscopy. A, Dimethyl sulfoxide (Control). B, Aphidicolin. C, Nocodazole. D, 7',8'-dehydropodophyllotoxin (**1**). E, 7',8'-dehydro acetyl podophyllotoxin (**2**). F, 7',8'-dehydro-*trans*-*p*-coumaroyl podophyllotoxin (**3**). Scale bar, 25 μm.

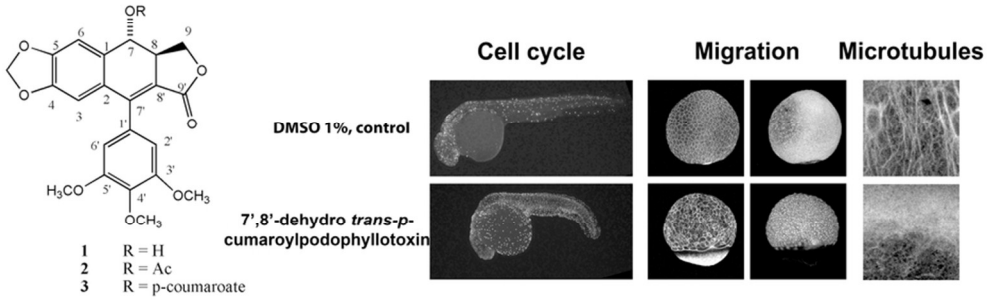

40x20mm (600 x 600 DPI)